Herwig Wendt, Patrice Abry, and Stéphane Jaffard

Bootstrap Methods in Signal Processing

Bootstrap for Empirical Multifractal Analysis

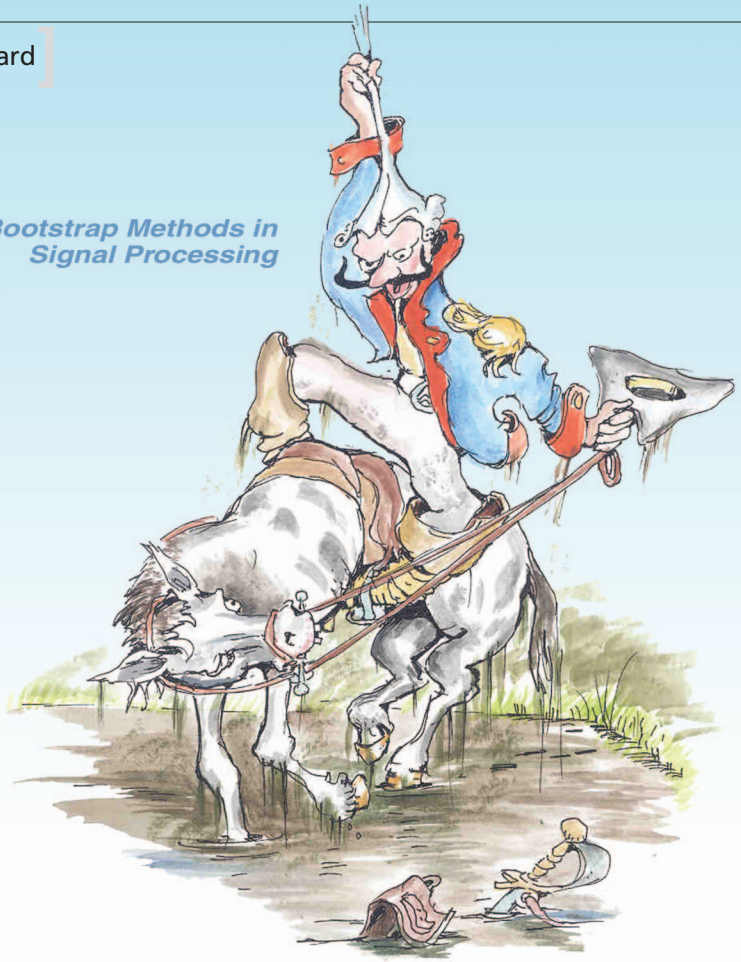

PROF. DR. KARL HEINRICH HOFMANN

Bootstrap application to hydrodynamic turbulence

Multifractal analysis is becoming a standard statistical analysis technique. In signal processing, it mostly consists of estimating scaling exponents characterizing scale invariance properties. For practical purposes, confidence intervals in estimation and p values in hypothesis testing are of primary importance. In empirical multifractal analysis, the statistical performance of estimation or test procedures remain beyond analytical derivation because of the theoretically involved nature of multifractal processes. Therefore, the goal of this article is to show how nonparametric bootstrap approaches circumvent such limitations and yield procedures that exhibit satisfactory statistical performance and can hence be practically used on real-life data. Such tools are illustrated at work on the analysis of the multifractal properties of empirical hydrodynamic turbulence data.

MOTIVATION: BOOTSTRAP FOR MULTIFRACTAL ANALYSIS?

SCALE INVARIANCE

The concept of scale invariance, or scaling, refers to systems or signals for which no scale of time or space can be identified as playing a characteristic role. Historically, scale invariance had been tied to $1/f$ spectrum for stochastic second-order stationary processes. However, it has been shown [1] that scale invariance can fruitfully be modeled with self-similar [2] and/or multifractal

1053-5888/07/$25.00©2007IEEE

[3] processes. This implies two major changes in paradigms [4]: First, the definition of scaling involves a whole range of statistical orders (positive, negative, and fractional), and not only the second one, as for the spectrum. Second, standard spectral estimates are replaced with multiresolution quantities, labeled $T_X(a, t)$, i.e., quantities describing the content of X (the process under analysis) around a time position t and a scale a. Standard examples for the $T_X(a, t)$ are given by wavelet, increment, or box-aggregated coefficients. Therefore, scale invariance is now commonly and operationally defined as the power law behaviors of the time average of the qth power of the $T_X(a, t)$ with respect to the analysis scale a for a given (large) range of scales $a \in [a_m, a_M]$, $a_M/a_m \gg 1$:

$$\frac{1}{n_a}\sum_{k=1}^{n_a} |T_X(a, k)|^q \simeq c_q a^{\zeta(q)}. \tag{1}$$

PRACTICAL SCALING ANALYSIS MOSTLY AMOUNTS TO MEASURING THE SCALING EXPONENTS $\zeta(q)$ FROM THE OBSERVED DATA.

PRACTICAL SCALING ANALYSIS

Practical scaling analysis mostly amounts to measuring the scaling exponents $\zeta(q)$ from the observed data. The estimated exponents are used for the physical understanding of the mechanisms producing the data or for standard signal processing tasks such as detection, identification, or classification. Scaling analysis, often referred to as multifractal analysis, is currently becoming a standard technique in statistical signal processing available in most up-to-date empirical data analyses toolboxes. It has been involved in a large variety of applications and in the analysis of data with very different nature, ranging from natural phenomena to human activities.

LIMITATIONS AND NEEDS IN PRACTICAL SCALING ANALYSIS

In real life applications, practical interest lies as much in the confidence that can be granted to an estimate as in the estimate itself. Equivalently, stronger inference can be drawn from hypothesis tests if they output not only decisions but also reliable p values or if their powers are known. Surprisingly, and despite its being widely used and increasingly popular, scaling analysis suffers here from a major difficulty: Little is known theoretically on the statistical performance of the scaling analysis procedures commonly used in practice, and essentially based on log-log plots, as suggested by (1). When X is a Gaussian self-similar process, the statistical performances can be studied theoretically and asymptotical results (in the limit of large observation durations) can be established (see, e.g., [4]–[7]). However, for multifractal processes, no theoretical statistical performance study is available, and little has been done empirically (see, a contrario, [8]). This is mainly due to the fact that most, if not all, stochastic multifractal processes practically used are defined from multiplicative martingales. The construction of such mathematical models is involved and results in strongly dependent and heavy tailed (hence strongly non-Gaussian) stochastic processes. The statistical performance of the analysis procedures hence turn out to be too difficult for analytical derivation. This implies that practitioners are lacking tools to assess the confidence they should grant to the obtained estimates. Along the same line, no hypothesis test validating the precise multifractal nature and properties of the data under analysis is available, while this issue is mentioned as crucial in most contributions where multifractal analysis is used. For instance, there is so far no statistical procedure available in the literature that enables us to decide whether real-life data are better described by monofractal self-similar processes [such as fractional Brownian motion (FBM)] or by truly multifractal processes. Also, practitioners often need to decide whether a simple multifractal model satisfactorily matches the data or if a more elaborate model is to be involved. Answering such questions is of major theoretical and practical importance. First, the inferred understanding of the phenomena producing the data under analysis may be dramatically changed. Self similar processes are deeply related to random walks and additive phenomena, while multifractal processes are historically tied to multiplicative structures. Second, for these different classes of models, both the number of parameters that need to be matched and the computational complexities that need to be handled are radically different. However, despite the huge collection of research articles describing the practical use of multifractal analysis on real-life data, the state-of-the-art tools to assess confidence in estimates and decision making remained, up to a recent past, the experience and eyes of the practitioners.

NONSTANDARD STATISTICAL TECHNIQUES

In this article, we illustrate how the use of nonstandard statistical techniques such as bootstrap may bring relevant solutions to overcome the difficulties mentioned above. The most recent and up-to-date theoretical developments (wavelet leaders) in multifractal analysis are first given a tutorial introduction. Bootstrap procedures applied to multiresolution quantities are then detailed. They aim at providing the practitioners with confidence intervals for multifractal attribute estimates and hypothesis tests for assessing the multifractal nature of the data under analysis. The effectiveness and benefits of these procedures are studied and illustrated on reference synthetic multifractal processes. We end up with a set of procedures that can be applied to a single observation of data with finite duration and that output not only estimates of multifractal attributes but also confidence intervals for theses estimates and not only the test decisions but also the p values obtained for a priori chosen null hypotheses.

HYDRODYNAMIC TURBULENCE

Hydrodynamic turbulence (cf. [9] for a review) is the scientific domain that gave birth to the concept of multifractal. The seminal works by Yaglom and Mandelbrot in the 1960s and 1970s indeed proposed to describe the celebrated Richardson energy cascade of turbulence flows by means of split and multiply iterative constructions. It has since been recognized that velocity or dissipation turbulence fields possess scale invariance properties and are well described with multifractal models. It remains, however, to decide whether a simple log-normal multifractal model or a more elaborate log-Poisson one better fits the data, an open and much controversial issue. Answering such a question is of theoretical importance as it may help to better understand the physical mechanisms at work in the development of turbulence flows. The bootstrap-based estimation procedures and hypothesis tests enable us to revisit this old question.

IN REAL LIFE APPLICATIONS, PRACTICAL INTEREST LIES AS MUCH IN THE CONFIDENCE THAT CAN BE GRANTED TO AN ESTIMATE AS IN THE ESTIMATE ITSELF.

MULTIFRACTAL ANALYSIS

MULTIFRACTAL SPECTRUM

Multifractal analysis describes the fluctuations along time t of the regularity of the sample path of a function $X(t)$. This is achieved by comparing the local variations of $X(t)$, around time position t_0, against a local power law behavior: $X(t_0)$ is said to belong to $C^\alpha(t_0)$ with $\alpha \geq 0$ if there exists a positive constant C and a polynomial P, satisfying $\deg(P) < \alpha$, such that $|X(t) - P_{t_0}(t)| \leq C|t - t_0|^\alpha$. The Hölder exponent is defined as the largest such α: $h(t_0) = \sup\{\alpha : X \in C^\alpha(t_0)\}$. The information regarding the variability of the regularity of $X(t)$ along t is usually described through the so-called singularity (or multifractal) spectrum $D(h)$. It is defined as the Hausdorff dimension of the set of points $\{t_k, k \in K\}$ on the real line, where the Hölder exponent takes the value h. For a detailed introduction to multifractal analysis, see [3] and [10]. A key practical issue consists of obtaining $D(h)$ from a single finite duration observation of data. This can be achieved using the wavelet leader multifractal formalism [10], [11].

WAVELET LEADER MULTIFRACTAL FORMALISM

WAVELET LEADERS

Let $\psi_0(t)$ be an elementary function, referred to as the mother-wavelet. It is characterized by its number of vanishing moments, a strictly positive integer $N_\psi \geq 1$, such that $\forall k = 0, 1, \ldots, N_\psi - 1$, $\int_{\mathbb{R}} t^k \psi_0(t)dt \equiv 0$, and $\int_{\mathbb{R}} t^{N_\psi} \psi_0(t)dt \neq 0$. Also, the collection of dilated and translated templates of ψ_0, $\{\psi_{j,k}(t) = 2^{-j/2}\psi_0(2^{-j}t - k), j \in \mathbb{Z}, k \in \mathbb{Z}\}$ form an orthonormal basis of $L^2(\mathbb{R})$. The discrete wavelet transform (DWT) of X is defined through its coefficients $d_X(j,k) = \int_{\mathbb{R}} X(t)\, 2^{-j}\psi_0(2^{-j}t - k)\, dt$ (cf. [12] for details on wavelet transforms).

Let us now further assume that $\psi_0(t)$ has a compact time support, and let us define dyadic intervals as $\lambda = \lambda_{j,k} = [k2^j, (k+1)2^j)$. Also, let 3λ denote the union of the interval λ with its two adjacent dyadic intervals: $3\lambda_{j,k} = \lambda_{j,k-1} \cup \lambda_{j,k} \cup \lambda_{j,k+1}$. Following [10], we define wavelet leaders as: $L_X(j,k) \equiv L_\lambda = \sup_{\lambda' \subset 3\lambda} |d_{X,\lambda'}|$. Hence, $L_X(j,k)$ consists of the largest wavelet coefficient $d_X(j',k')$ computed at all finer scales $2^{j'} \leq 2^j$ within a narrow time neighborhood $(k-1)\cdot 2^j \leq 2^{j'}k' < (k+2)\cdot 2^j$. In all cases and for all processes, under mild regularity conditions on X, wavelet leaders exactly reproduce the Hölder exponent of X at t_0: $h(t_0)$ is the supremum of the values h such that $L_X(j,k) \leq C2^{jh}$ is verified in the limit of fine scales ($2^j \to 0$) and for j,k such that $2^j k = t_0$ [10]. The general validity of this local power law behavior is the key property ensuring the validity and relevance of the multifractal formalism developed in the following.

MULTIFRACTAL FORMALISM

For fixed analysis scales $a = 2^j$, the time averages of (the qth powers of) the $L_X(j,k)$ are referred to as the structure functions (with n_j the number of $L_X(j,k)$ available at scale 2^j): $S^L(j,q) = (1/n_j)\Sigma_{k=1}^{n_j} L_X(j,k)^q$. Following developments in [13] and intuitions based on the fact that wavelet leaders reproduce exactly Hölder regularity, it can be shown [10], [11] that, under mild uniform Hölder regularity condition on $X(t)$,

$$S^L(j,q) = F_q 2^{j\zeta(q)}, \tag{2}$$

in the limit $2^j \to 0$. Moreover, the Legendre transform of the scaling exponents $\zeta(q)$ provides an upper bound for the multifractal spectrum $D(h) \leq \min_{q \neq 0}(1 + qh - \zeta(q))$. This inequality turns into an equality for most commonly used multifractal models. Hence, the multifractal formalism consists of obtaining $D(h)$ from the measurement of the $\zeta(q)$.

LOG CUMULANTS

The $S^L(j,q)$, consisting of time averages, can be read as sample mean estimators for the ensemble averages $\mathbb{E}L_X(j,\cdot)^q$. This heuristic analysis was first proposed using increments in [14] and further developed for continuous wavelet coefficients in [15]. We further extend this interpretation to wavelet leaders. Hence, (2) is rewritten as $\mathbb{E}L_X(j,\cdot)^q = F_q 2^{j\zeta(q)}$. When $\mathbb{E}L_X(j,\cdot)^q$ is finite, a standard generating function expansion yields: $\ln \mathrm{E}e^{q \ln L_X(j,\cdot)} = \sum_{p=1}^{\infty} C^L(j,p)(q^p/p!)$, where $C^L(j,p)$ stands for the cumulants of order $p \geq 1$ of the $\ln L_X(j,\cdot)$. Combining the equations above compels $C^L(j,p)$ to satisfy the following scale dependence:

$$\forall p \geq 1,\ C^L(j,p) = c_{0,p} + c_p \ln 2^j \tag{3}$$

and yields $\zeta(q) = \sum_{p=1}^{\infty} c_p (q^p/p!)$. The knowledge of the $\zeta(q)$ (and therefore of $D(h)$) can hence be rephrased in terms of the log cumulants c_p. More specifically, c_1 mostly characterizes the location of the maximum of $D(h)$, c_2 its width and c_3 its asymmetry. The triplet (c_1, c_2, c_3) thus gathers most of the multifractal information practically available from empirical data. For practical purposes, approximating the functions $\zeta(q)$ or $D(h)$ with a limited number of c_p can hence significantly ease the classification or detection tasks based on multifractal (MF) attributes.

MONO- VERSUS MULTIFRACTAL

A crucial question in applications lies in deciding whether the data should be described by a monofractal process [2], or with multifractal models. For the former, if the multifractal formalism holds (which is the case for Gaussian self-similar processes with stationary increments), then $\zeta(q) = qH$ and hence $\forall p \geq 2 :\ c_p \equiv 0$, while for most multifractal processes of interest, $c_2 \neq 0$. This is where estimating precisely c_2 and testing $c_2 = 0$ or not, is useful.

WAVELET LEADERS VERSUS WAVELET COEFFICIENTS

Previous multifractal formalisms, based on increments or wavelet coefficients instead of wavelet leaders, fail to provide the practitioners with a correct analysis of the entire multifractal spectrum and do not generally hold, even for standard processes such as FBMs. In contrast, the wavelet leader multifractal formalism holds for most multifractal processes of practical interest and gives access to their entire multifractal spectrum [11]. Another multifractal formalism based on the skeleton of the continuous wavelet transform has been previously proposed and is also commonly used in the context of turbulence, (see, e.g., [16]). For a detailed analysis of the theoretical and practical relevance and benefits of the use of wavelet leaders for multifractal analysis, see [8], [10], and [11].

MULTIFRACTAL PARAMETER ESTIMATION

Empirical multifractal analysis mostly consists of estimating the $\zeta(q)$ or the c_p. Equations (2) and (3) suggest that estimations are to be performed by means of linear regressions in $\log_2 2^j = j$ versus $\log_2 S^L(j,q)$ and $\ln 2^j$ versus $C^L(j,q)$ coordinates, respectively.

$$\hat{\zeta}(q) = \sum_{j=j_1}^{j_2} w_j \log_2 S^L(j,q), \tag{4}$$

$$\hat{c}_p = (\log_2 e) \cdot \sum_{j=j_1}^{j_2} w_j \hat{C}^L(j,p), \tag{5}$$

where the estimates $\hat{C}^L(j,p)$ for the cumulants of $\ln L_X(j,\cdot)$ are obtained from standard sample cumulant estimators. To estimate the multifractal spectrum, we can use a parametric formulation, proposed in [17], that avoids the computation of the Legendre transform:

$$\hat{D}(q) = \sum_{j=j_1}^{j_2} w_j U^L(j,q), \qquad \hat{h}(q) = \sum_{j=j_1}^{j_2} w_j V^L(j,q), \tag{6}$$

where $U^L(j,q) = \Sigma_{k=1}^{n_j} R_X^q(j,k) \log_2 R_X^q(j,k) + \log_2 n_j$, $V^L(j,q) = \Sigma_{k=1}^{n_j} R_X^q(j,k) \log_2 L_X(j,k)$ and $R_X^q(j,k) = L_X(j,k)^q / \Sigma_{k=1}^{n_j} L_X(j,k)^q$.

The weights w_j have to satisfy the constraints $\Sigma_{j_1}^{j_2} j w_j \equiv 1$ and $\Sigma_{j_1}^{j_2} w_j \equiv 0$ and can be expressed as $w_j = b_j((V_0 j - V_1)/(V_0 V_2 - V_1^2))$ with $V_i = \Sigma_{j_1}^{j_2} j^i b_j$, $i = 0, 1, 2$. The freely selectable positive numbers b_j reflect the confidence granted to each $\hat{C}^L(j,p)$ or $\log_2 S^L(j,q)$. Following [4], we perform weighted ($b_j = n_j$) or nonweighted ($b_j = 1$) linear fits.

BOOTSTRAP AND MULTIFRACTAL ANALYSIS

Standard methods for estimating confidence limits and null distributions are based on Gaussian theory. For instance, for Gaussian self-similar processes, asymptotic expansions for confidence intervals of scaling exponents have been derived [4], [7]. However, such approximations perform poorly when applied to multifractal processes because of their non-Gaussian nature. Practical multifractal analysis demands robust statistical techniques such as nonparametric bootstrap; indeed, the aim of nonparametric bootstrap is to compensate for the fact that little, if not nothing, is known about the models underlying the analyzed data besides their possessing some form of scale invariance.

NONPARAMETRIC BOOTSTRAP

In a nutshell, nonparametric bootstrap makes use of the empirical distribution, obtained from the available sample, to approximate the unknown population distribution from which the sample is drawn. This empirical distribution is then used to estimate the distribution of the estimators of the targeted population parameters. More precisely, a collection of resamples is constructed, each resample being drawn with replacement from the original sample. Then the estimates are calculated for each resample, and hence, their empirical distributions can be estimated (see, e.g., [18] and [19]).

BLOCK BOOTSTRAP

The simple nonparametric bootstrap procedure needs to be adapted if the sample $\mathcal{X}$ is not independent identically distributed (i.i.d.) but correlated. Then, rather than drawing a single observation at a time, blocks of observations of length l are drawn randomly with replacement. This ensures that the dependence structure of the original observations is preserved within each block. Among the various block bootstrap methods, the popular moving blocks and circular block bootstrap belong to the most performant ones in many situations [20]. They are based on overlapping blocks $\mathcal{B}_i = \{X_i, \ldots, X_{i+l-1}\}$, $i = 1, \ldots, n-l+1$ of fixed size l. The circular block bootstrap uses additional periodically extended blocks at the end of the sample, ensuring that the same weight is assigned to all observations. This latter choice is used in the multifractal analysis resampling scheme described below.

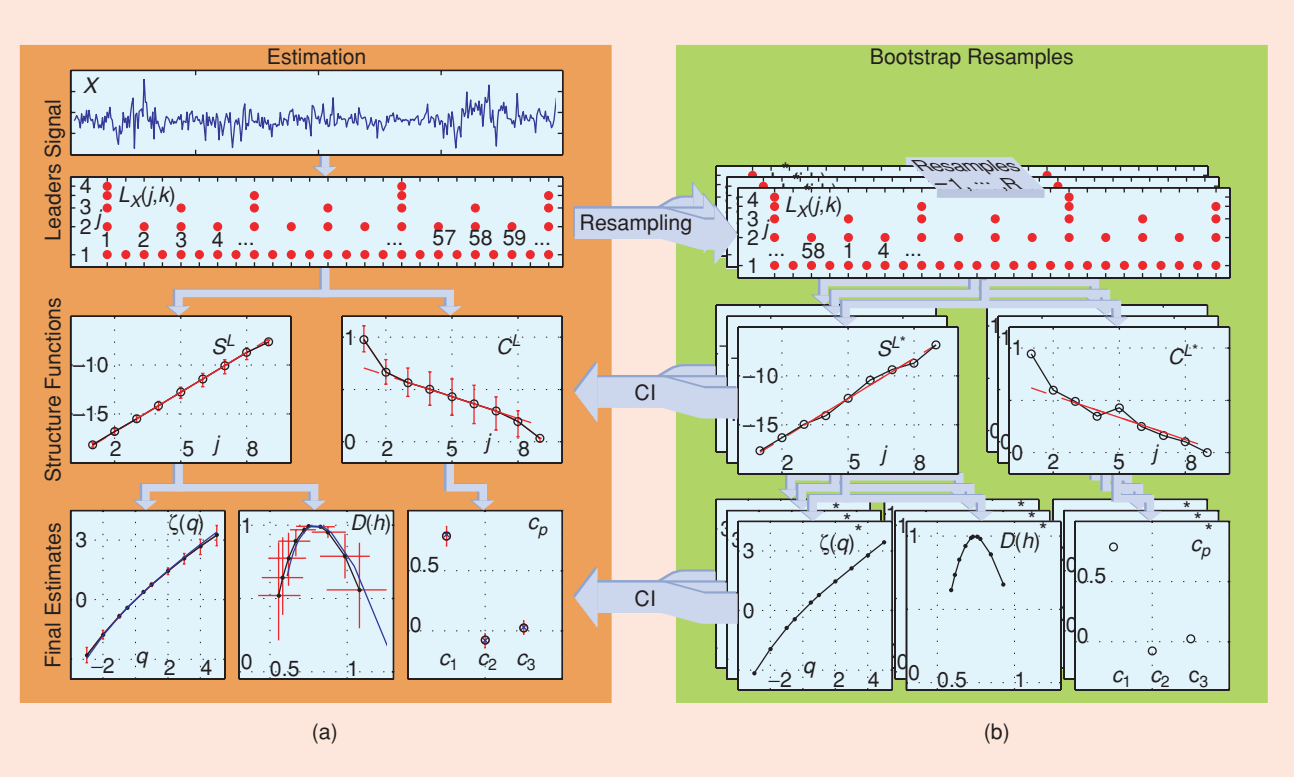

[FIG1] Bootstrap-based multifractal parameter estimation with confidence intervals scheme. (a) From the data, the wavelet leaders are computed (top). From the wavelet leaders, structure functions $S^L(j,q)$ and $C^L(j,p)$ (middle) and the corresponding estimates for the multifractal parameters $\Theta \in \{\zeta(q), D(q), h(q), c_p\}$ (bottom) are obtained. (b) At each scale independently, the wavelet leaders are block bootstrapped (top). From these R resamples, confidences intervals for $S^L(j,q)$ and $C^L(j,p)$ (middle) and for the multifractal attributes (bottom) are obtained and reported on the original estimates (in red).

RESAMPLING SCHEME

The bootstrap procedure, adapted for multifractal analysis, is illustrated in Figure 1, together with the estimation procedures described in the previous section: At first, the wavelet leaders $\mathcal{L}_j = \{L_X(j,1), \ldots, L_X(j,n_j)\}$, $j = 1, \ldots, j_{\max}$ are calculated from the sample X. Then, at each scale j, R bootstrap resamples $\mathcal{L}_j^{*(1)}, \ldots, \mathcal{L}_j^{*(R)}$ are generated from the original sample of leaders $\mathcal{L}_j$. Each resample $\mathcal{L}_j^{*(r)} = \{L_X^{*(r)}(j,1), \ldots, L_X^{*(r)}(j,n_j)\}$ is an unsorted collection of n_j sample points, drawn blockwise and with replacement from the original sample $\mathcal{L}_j$. For each resample, the R bootstrap structure functions $\{S^{L*(r)}(j,q)\}_{r=1}^R$, $\{U^{L*(r)}(j,q)\}_{r=1}^R$, $\{V^{L*(r)}(j,q)\}_{r=1}^R$ and $\{C^{L*(r)}(j,p)\}_{r=1}^R$ are calculated. Finally, we obtain the R bootstrap estimates by plugging-in the bootstrap structure function estimations in (4)–(6).

BLOCK SIZE

An optimal block length l exists that theoretically depends jointly on the correlation, the length of the sample, and the definition of the estimator itself (cf. [20]). In the case of DWTs, correlation among wavelet coefficients remains significant over an interval whose size is of the order of magnitude of the time support of the mother wavelet M_ψ and then decreases exponentially. By construction of the DWT, the length of the sample $n_j \approx n \cdot 2^{-j}$ is different at each scale j. Therefore, the optimal block length at each scale should be different. Numerical simulations show that fixing the same block length $l_j = l$ rather than choosing the optimal block length for each sample size n and scale j has only very little impact on the performance of the bootstrap estimators as soon as $l \geq M_\psi$. We therefore fix $l = M_\psi$ for each scale j and sample size n (for the Daubechies wavelets used here: $M_\psi = 2 \cdot N_\psi$).

BOOTSTRAP CONFIDENCE LIMITS

The empirical distributions of the bootstrap estimates are used to approximate the distributions of the estimators in (4)–(6) and hence for constructing confidence limits for these quantities.

PERCENTILE LIMITS

The equitailed $(1-\alpha)$ percentile confidence limit for the parameter $\Theta \in \{\zeta(q), D(q), h(q), c_p\}$ is defined as

$$\left[\hat{\Theta}^*_{\frac{\alpha}{2}};\ \hat{\Theta}^*_{(1-\frac{\alpha}{2})}\right].$$

Here, $\hat{\Theta}^*_\alpha$ is the α quantile of the empirical distribution of $\hat{\Theta}^*$, the bootstrap equivalents of (4)–(6).

STUDENTIZING

If accurate standard deviation estimates for $\hat{\Theta} \in \{\hat{\zeta}(q), \hat{D}(q), \hat{h}(q), \hat{c}_p\}$ are available, confidence limits

based on the distribution of the studentized parameter $\hat{\Psi} = (\hat{\Theta} - \Theta)/\hat{\sigma}^*$, are intrinsically more accurate (cf. [19]). Here $\hat{\sigma}^*$ is the bootstrap standard deviation of $\hat{\Theta}$ estimated on the resamples $\hat{\Theta}^*$. The bootstrap approximation to the studentized distribution is given by the empirical distribution of $\hat{\Psi}^{*(r)} = (\hat{\Theta}^{*(r)} - \hat{\Theta})/(\hat{\sigma}^{**(r)}),\ r = 1, \ldots, R,$ where $\hat{\sigma}^{**(r)} = \text{Std}^{**}\hat{\Theta}^{**(r,s)}$ are the bootstrap standard deviation estimates of $\hat{\Theta}^{*(r)}$ obtained from S double bootstrap estimates $\hat{\Theta}^{**(r,s)},\ s = 1, \ldots, S$. The $(1-\alpha)$ studentized confidence limit for Θ is defined as

$$\left[\hat{\Theta} - \hat{\sigma}^*\hat{\Psi}^*_{(1-\frac{\alpha}{2})};\ \hat{\Theta} - \hat{\sigma}^*\hat{\Psi}^*_{\frac{\alpha}{2}}\right],$$

where $\hat{\Psi}^*_\alpha$ is the α quantile of the empirical distribution of the studentized variable $\hat{\Psi}^*$.

ESTIMATION FROM A SINGLE OBSERVATION

The procedures (estimates and confidence intervals) can be applied to a single observation of data with finite (possibly short) duration, as illustrated in Figure 1(a) and Figure 2 with synthetic processes and hydrodynamic turbulence data, respectively.

BOOTSTRAP HYPOTHESIS TESTS

TESTS ON LOG CUMULANTS

As discussed previously, key issues in practical multifractal analysis consist of deciding whether monofractal or multifractal processes better match the data and whether simple ($c_p \equiv 0,\ p \geq 3$) or more elaborate multifractal models are preferred. As detailed previously, the log cumulants c_1, c_2, c_3, provide us with central attributes to quantify the multifractal nature of the data. Therefore, being able to perform statistical tests on c_p constitutes a major step to address such issues. We study hypothesis tests of the form $H_0 : c_p = c_{p,0}$ against the double-sided alternative $c_p \neq c_{p,0}$. The tests are based on the basic and on the studentized test statistics

$$\hat{t}_B = \hat{c}_p - c_{p,0}, \quad \hat{t}_S = \frac{\hat{c}_p - c_{p,0}}{\hat{\sigma}^*}. \tag{7}$$

STATISTICAL TESTS

A significance $(1-\alpha)$ test rejects H_0 when the probability of observing $\hat{t}$ under the hypothesis is smaller than α. More precisely, the test d_α reads $d_\alpha = 1$ if $\hat{t} \notin \mathcal{T}_{(1-\alpha)}$ and $d_\alpha = 0$, otherwise, where the acceptance region $\mathcal{T}_{(1-\alpha)}$ is defined as $\Pr\{t \in \mathcal{T}_{(1-\alpha)} | P_t^{H_0}\} = 1 - \alpha$. A good test should have both low probability of rejecting H_0 when it is true, and high probability when H_0 is false. The former is the significance α and is usually, in practice, set a priori. The probability of rejecting $H_0 : c_p = c_{p,0}$ when it is false is called the power β of the test against a specific true alternative $c_{p,A}$. The p-value p of an observation $\hat{t}$ is defined as the critical value α for which $\hat{t}$ would be regarded as just decisive against H_0 and quantifies the plausibility of rejecting H_0 having observed $\hat{t}$ (see e.g., [21] for more details on tests).

BOOTSTRAP TESTS

The distribution of the test statistic under H_0, $P_t^{H_0}(\tau) = \Pr(t < \tau | H_0)$, is unknown in most situations and in practice often approximated by parametric models. Due to the lack of knowledge on the statistical properties of multiresolution quantities for multifractal processes, the nonparametric bootstrap scheme described previously is used to obtain estimations of the null distribution of $\hat{t}$. They are given by the empirical distributions of $\hat{t}^*_B$ and $\hat{t}^*_S$ [22]–[24]

$$\left\{\hat{t}^{*(r)}_B = \hat{c}^{*(r)}_p - \hat{c}_p\right\}_{r=1}^{R},\ \left\{\hat{t}^{*(r)}_S = \frac{\hat{c}^{*(r)}_p - \hat{c}_p}{\hat{\sigma}^{**(r)}}\right\}_{r=1}^{R}.$$

The approximate acceptance regions are now constructed from the quantiles of these estimated distributions

$$\widehat{\mathcal{T}}^{per}_{(1-\alpha)} = \left[-\hat{t}^*_{B(1-\frac{\alpha}{2})}, -\hat{t}^*_{B(\frac{\alpha}{2})}\right],\ \widehat{\mathcal{T}}^{stu}_{(1-\alpha)} = \left[\hat{t}^*_{S,(\frac{\alpha}{2})}, \hat{t}^*_{S,(1-\frac{\alpha}{2})}\right].$$

Plugged into the bootstrap test formulation, they give rise to the percentile and the studentized bootstrap test, respectively.

OTHER TESTS AND CONFIDENCE LIMITS

There exists a variety of bootstrap tests and confidence limits (see e.g., [23], [24]). We chose the percentile and studentized constructions as one representative of simple and double bootstrap methods. The detailed performance of various bootstrap tests were carefully compared in the context of multifractal analysis in [8]. Generally, double bootstrap methods are asymptotically more accurate, at the price, however, of a computational load increase by a factor $\approx S$ when applied naively, which may not be acceptable in numerous practical situations.

STRUCTURE FUNCTIONS CONFIDENCE LIMITS: REGRESSION RANGE SELECTION

A key issue in practical multifractal analysis remains the selection of an appropriate range of scales for the regressions (4)–(6). As with real-life empirical data, scaling properties are likely to exist only over a finite range of scales. This selection is usually performed by eyes by practitioners. The empirical distributions of the bootstrap structure functions can be used to construct confidence limits for the structure functions $S(j, q)$ and $C(j, p)$, in similar ways as confidence limits for the estimates themselves (cf. Figure 1). Such confidence limits can help the practitioner in selecting the operational scaling range by choosing the scales for which the regression line lies within confidence intervals. This is the first step toward a true goodness-of-fit statistical test, an issue currently under analysis. To illustrate the regression range selection issue, Figure 1(a) and Figure 2(a) and (b) show structure functions together with percentile bootstrap confidence limits obtained from a single observation of a synthetic multifractal process and real hydrodynamic data, respectively.

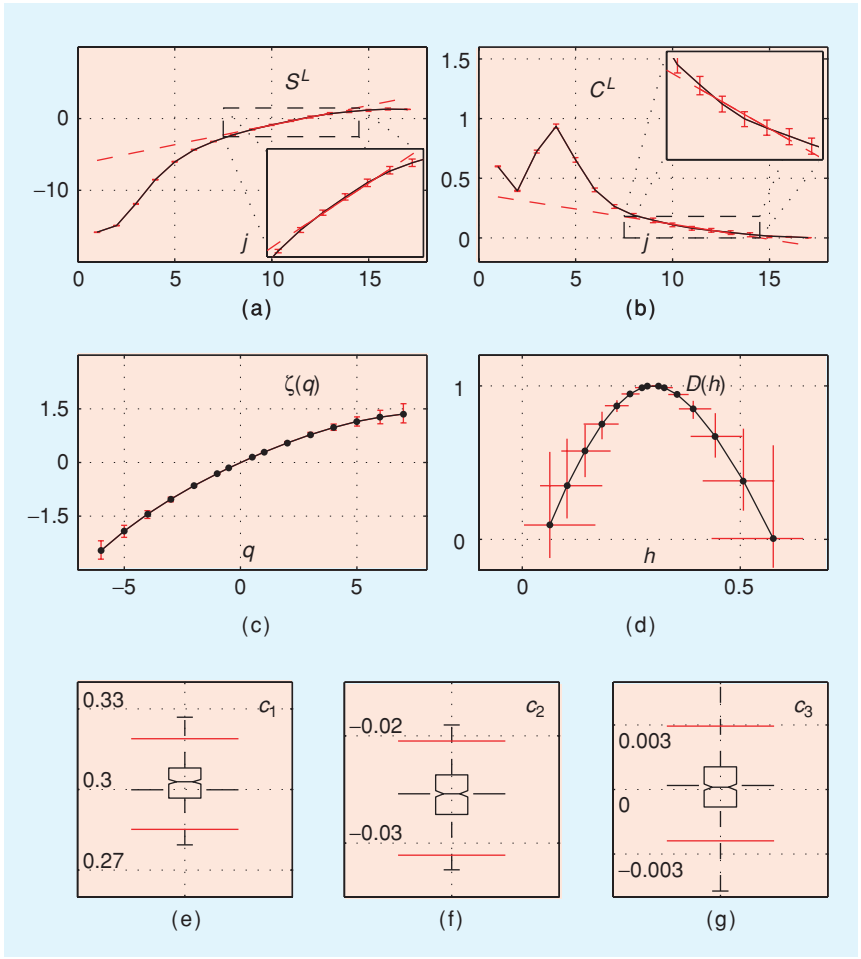

[FIG2] Multifractal analysis of Turbulence data. (a) Structure functions (q = 2) and (b) cumulant estimates (p = 2) for a single run of Jet Turbulence data ($n = 2^{20}$). The confidence limits confirm the choice of regression range, $j = 9 - 13$. (c) Estimates (in solid black) of scaling exponent $\zeta(q)$, (d) multifractal spectrum $D(h)$, and (e)–(g) log cumulants log c_p. The boxplots are obtained on $\hat{c}_p^*$ and show the lower and upper quartile, median, and support of their empirical distributions. All bootstrap confidence limits (in red) are obtained with the percentile method ($\alpha = 0.05$).

BOOTSTRAP MULTIFRACTAL ANALYSIS: STATISTICAL PERFORMANCE

SYNTHETIC MULTIFRACTAL PROCESSES

To assess the statistical performance of the proposed bootstrap procedures, we apply them to three different types of stochastic processes with a priori known and controlled scaling and multifractal properties, FBM [2], Multifractal random walk (MRW) [25] and FBM in compound Poisson motion (CPM) multifractal (MF) time (CPM-MF-FBM) [26]. These three processes are chosen for their being representative of large classes of situations: FBM is a Gaussian monofractal process, $c_p = 0, \forall p \geq 2$, while MRW and CPM-MF-FBM are non-Gaussian heavy tail multifractal processes. The pair FBM/MRW can be used to validate estimation and hypothesis tests related to nonzero c_2 while MRW/CPM-MF-FBM enables to assess the relevance of the estimation and hypothesis tests for nonzero c_3, as for MRW $c_p = 0, \forall p \geq 3$. To the best of our knowledge, this last issue has never been addressed in the literature.

ESTIMATION PROCEDURES

SIMULATION SETUP

The results presented here are obtained using Daubechies wavelets with $N_\psi = 3$, sample size $n = 2^{15}$, $N_{MC} = 1{,}000$ and $b_j = n_j$. The bootstrap parameters are fixed to $l = 2 \cdot N_\psi = 6$, and $R = 399$, $S = 50$. The nominal significance is chosen to be $\alpha = 0.05$. Parameters (c_1, c_2, c_3) for the three processes have been varied over wide ranges.

PERFORMANCE OF PARAMETER ESTIMATORS

The performance of the estimators in (4)–(6), $\hat{\Theta} \in \{\hat{\zeta}(q), \hat{D}(q), \hat{h}(q), \hat{c}_p\}$, are quantified by their (root) mean squared error (MSE) ($\widehat{\mathrm{Var}}_{N_{MC}}$ and $\widehat{\mathbb{E}}_{N_{MC}}$ stand for the sample variance and sample mean estimates obtained from N_{MC} independent realizations)

$$\mathrm{MSE}_{N_{MC}}^{\hat{\Theta}} = \sqrt{\widehat{\mathrm{Var}}_{N_{MC}}\hat{\Theta} + (\widehat{\mathbb{E}}_{N_{MC}}\hat{\Theta} - \Theta)^2}.$$

MSE results are compared in Table 1 (obtained from CPM-MF-FBM). For negative q, wavelet coefficient-based estimators exhibit very large MSEs and are not meaningful: Hence, they can not capture the entire multifractal spectrum of the analyzed process. Moreover, compared to wavelet coefficient-based estimates, wavelet leader estimates exhibit significant MSE gains for the estimations of the c_p, $p \geq 2$ (i.e., for the parameters measuring the discrepancies between mono- and multifractality). This clearly indicates that, while the estimation of self-similar attributes can satisfactorily be conducted with wavelet coefficients, multifractal attribute estimations require the use of wavelet leaders to be reliable. Note moreover that, to the best of our knowledge, it has never been shown before in the literature that a nonzero c_3 can be correctly estimated.

COVERAGE OF BOOTSTRAP CONFIDENCE INTERVALS

The reliability of the percentile and the studentized confidence limits CI_Θ for $\Theta \in \{\zeta(q), D(q), h(q), c_p\}$ are evaluated through their empirical coverage: $\mathrm{Cover}_{N_{MC}}^{\hat{\Theta}} = \widehat{\mathrm{E}}_{N_{MC}}\mathrm{I}\{\Theta \in \widehat{\mathrm{CI}}_\Theta\}$, where $\mathbb{I}\{\cdot\}$ is the indicator function of the event $\{\cdot\}$. Thus, the empirical coverage consists of the estimated probability that the parameter Θ lies in the estimated confidence region. Results in Table 1 clearly show that the

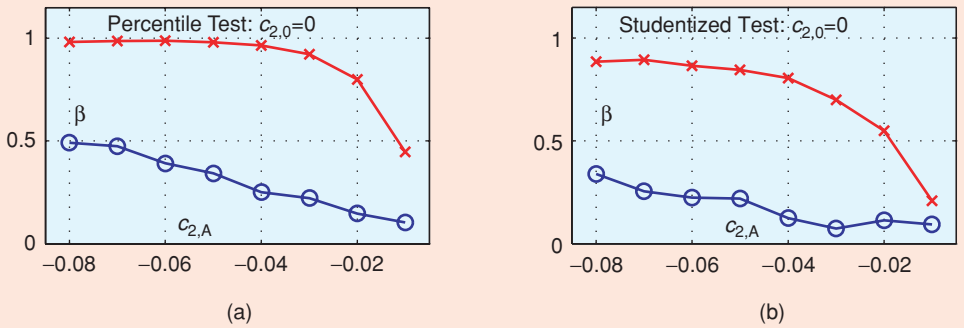

[FIG3] Powers of $c_{2,0} = 0$ against $c_{2,A} \neq 0$. (a) Powers $\hat{\beta}_{N_{MC}}$ of percentile and (b) studentized tests of $c_{2,0} = 0$ against multiple alternatives $c_2 = c_{2,A}$ for MRW (blue circles: wavelet coefficients—red crosses: wavelet leaders).

leader-based bootstrap confidence limits closely reproduce the target coverage of 95% and are thus highly reliable. The coefficient-based confidence limits have similar performance, with the exception of estimates for negative q. The calculation intensive studentized limits do not perform better than the percentile limits.

HYPOTHESIS TESTS

SIGNIFICANCE OF BOOTSTRAP TESTS

The actual significance of the tests are estimated as $\hat{\alpha}_{N_{MC}} = \widehat{\mathbb{E}}_{N_{MC}}\{\hat{d}_\alpha | c_p = c_{p,0}\}$ and should ideally equal the preset significance α. Results obtained for CPM-MF-FBM are summarized in Table 2. We observe that for both leaders and coefficients and for tests on both c_2 and c_3, the actual significance of $\alpha = 0.05$ is reproduced closely. This indicates that the nonparametric bootstrap null distribution estimates $\hat{t}_B^{*(r)}$ and $\hat{t}_S^{*(r)}$ are valid approximations to the real null distributions of the test statistics.

POWER OF BOOTSTRAP TESTS

The power of the tests on $H_0 : c_p = c_{p,0}$ against a certain alternative $c_{p,A} \neq c_{p,0}$ are estimated as $\hat{\beta}_{N_{MC}}(c_{p,A}, \alpha) = \widehat{\mathbb{E}}_{N_{MC}}\{\hat{d}_\alpha | c_p = c_{p,A}\}$ and the larger, the better. With $p = 2$, the test essentially aims at rejecting self-similarity in favor of multifractality. The power of the tests $H_0 : c_2 = 0$ against the alternatives $c_{2,A} = \{-0.08, -0.07, \ldots, -0.01\}$ is assessed using MRW. Results are shown in Figure 3 and indicate that the leader-based tests have consistently much larger powers than the coefficient-based tests. Hence, whereas a wavelet

[TABLE 1] ESTIMATION PERFORMANCE AND CONFIDENCE INTERVAL COVERAGE. TRUE VALUE (LEFT COLUMN) AGAINST WAVELET COEFFICIENT (d_X) AND WAVELET LEADER (L_X) ESTIMATES TOGETHER WITH THEIR (ROOT) MEAN SQUARED ERROR MSE AND EMPIRICAL COVERAGES FOR THE PERCENTILE AND STUDENTIZED CONFIDENCE INTERVALS. THE TARGETED COVERAGE IS 95% AND IS SATISFACTORILY REPRODUCED FOR L_X.

		d_X			L_X		
	TRUE	**EST (MSE)**	**PER**	**STU**	**EST (MSE)**	**PER**	**STU**
$\zeta(-1)$	−0.85	−0.95 (0.27)	84	87	−0.83 (0.02)	92	97
$D(-1)$	0.95	0.56 (0.62)	68	80	0.95 (0.02)	86	88
$h(-1)$	0.90	1.40 (0.87)	74	83	0.88 (0.03)	88	92
$\zeta(+1)$	0.77	0.76 (0.01)	98	99	0.76 (0.01)	94	99
$D(+1)$	0.97	0.97 (0.01)	95	97	0.97 (0.01)	95	96
$h(+1)$	0.73	0.73 (0.02)	96	99	0.73 (0.02)	91	98
c_1	0.80	0.80 (0.02)	98	99	0.79 (0.02)	94	98
c_2	−0.08	−0.08 (0.04)	93	95	−0.07 (0.02)	95	96
c_3	0.03	0.05 (0.26)	90	93	0.03 (0.09)	90	94

[TABLE 2] SIGNIFICANCE AND POWERS OF WAVELET COEFFICIENT AND LEADER-BASED BOOTSTRAP TESTS. BOTH FOR c_2, c_3, LEADER-BASED TEST POSSESS SIGNIFICANTLY LARGER POWERS. THE NOMINAL SIGNIFICANCE IS $\alpha = 0.05$ AND IS SATISFACTORILY REPRODUCED.

	$c_2 = -0.08$				$c_3 = 0.0311$			
	d_X		L_X		d_X		L_X	
	PER	**STU**	**PER**	**STU**	**PER**	**STU**	**PER**	**STU**
$c_{p,0} = c_p$, $\hat{\alpha}_{N_{MC}}$	0.07	0.05	0.05	0.05	0.10	0.10	0.07	0.06
$c_{p,0} = 0$, $\hat{\beta}_{N_{MC}}$	0.57	0.40	1.00	0.96	0.13	0.11	0.39	0.28

[TABLE 3] MULTIFRACTAL PARAMETER ESTIMATES FOR TURBULENCE DATA. JET TURBULENCE (LEFT) AND WIND TUNNEL TURBULENCE (RIGHT) WAVELET-LEADER-BASED ESTIMATES OF LOG CUMULANTS c_p, TOGETHER WITH 95% BOOTSTRAP CONFIDENCE LIMITS. THE RESULTS ARE AVERAGED OVER RUNS.

	JET TURBULENCE DATA			WIND TUNNEL DATA		
p	1	2	3	1	2	3
$\hat{c}_p$	0.304	−0.021	−0.000	0.352	−0.026	0.001
LOW_{per}	0.287	−0.026	−0.002	0.342	−0.029	−0.001
HIGH_{per}	0.321	−0.016	0.002	0.361	−0.022	0.002
LOW_{stu}	0.284	−0.026	−0.002	0.341	−0.030	−0.001
HIGH_{stu}	0.326	−0.014	0.002	0.362	−0.022	0.003

coefficient-based multifractal analysis would have poor performance in detecting that the analyzed data do depart from a monofractal model, a wavelet leader-based analysis rejects H_0 with high probability, even in situations where the alternative is close to the null value [8].

The power of a test postulating that $c_3 = 0$ is estimated by applying it to realizations of CPM-MF-FBM, for which $c_3 = c_{3,A} = 0.0311 \neq 0$. Results, reported in Table 2, show that wavelet leader-based tests are much more powerful than wavelet coefficient-based tests, hence allowing satisfactory detection of true departure from zero values for c_3. Complementary results for estimations and tests can be found in [8].

CONCLUSIONS

The results obtained from the numerical simulations described here as well as the more complete results reported in [8] yield a number of conclusions. First, besides being mathematically well-grounded with respect to multifractal analysis, wavelet leaders exhibit significantly enhanced statistical performance compared to wavelet coefficients. This is notably true for the parameters controlling the difference between monofractal self-similar Gaussian and multifractal non-Gaussian processes, such as scaling exponents with negative statistical orders q or log cumulants c_p with $p \geq 2$. Second, bootstrap procedures provide practitioners with satisfactory confidence limits and hypothesis test p-values for multifractal parameters. Third, the computationally cheap percentile method achieves already excellent performance for both confidence limits and tests. It may thus be preferred over studentized or other double bootstrap methods in empirical multifractal analysis, when computation time is critical. In conclusion, combining the theoretically recommended and statistically efficient wavelet leader multifractal analysis with bootstrap procedures provides the practitioner with an empirical multifractal analysis toolbox enabling to estimate multifractal attributes, to provide (bootstrap-based) confidence intervals for these estimates and hypothesis tests for the values of these parameters, and hence to assess the multifractal properties of real-world empirical data. There are two key practical contributions. These procedures can be applied to a single observation of data with finite (possibly short) duration; they output not only multifractal parameter estimates and test decisions, but also estimated confidence limits and p-values.

MULTIFRACTAL ANALYSIS IN HYDRODYNAMIC TURBULENCE

TURBULENCE AND SCALING: A SHORT SURVEY

After the early work of Richardson in the 1920s, the heuristic understanding of hydrodynamic turbulence relates the erratic behaviors of most natural flows to a transfer of energy from large to small flow scales. This celebrated energy cascade-based heuristic analysis of turbulence flows is deeply associated with scale invariance. Between a coarse scale (where energy is injected by an external forcing) and a fine scale (where energy is dissipated by viscous friction), no characteristic scale can be identified. It led to the use of stochastic processes with built-in scale invariance properties for turbulence modeling. In 1941, Kolmogorov proposed the first stochastic description of turbulence based on FBM, hence on a monofractal model. However, after the seminal work by Yaglom, the energy transfer has often been modeled via split/multiply iterative random procedures, which match the physical intuitions beyond the vorticity stretching mechanisms at work in turbulence flows. Mandelbrot in the 1970s fruitfully gathered these models in the unified framework of multiplicative martingales and studied their properties [1]. Nowadays most practitioners agree on the existence of scale invariance in turbulence data and, following the analyses of Parisi and Frisch [27], on its multifractal nature. However, a major open issue consists of deciding which particular multifractal process better models turbulence flows. A large variety of cascades has been proposed over the last 30 years, each trying to better fit experimental data and/or to better account for a specific fluid flow property and yielding a different prediction for the multifractal spectrum. Let us concentrate on two among the most popular such models. In 1962, Obukhov and Kolmogorov proposed a model mostly based on a law of large numbers argument and referred to as the log-normal multifractal model (predicting $c_p \equiv 0$ for $p \geq 3$). More recently, She and Lévêque proposed an alternative construction relying on the key assumption that energy dissipation gradients must remain finite within turbulence flows, referred to as the log-Poisson model (predicting $\forall p: \; c_p \neq 0$). Discriminating between the log-normal and log-Poisson models hence requires the use of tools providing us with an accurate estimate for the c_3 parameter and with a statistical test

aiming at rejecting the null-hypothesis $c_3 \equiv 0$. For the log-normal and log-Poisson models, the canonical values for (c_2, c_3) are $(-0.0250, 0)$ and $(-0.0365, 0.0049)$, respectively (cf. Table 4). For thorough introductions to turbulence, see [9] and [28].

DATA DESCRIPTION

In this article, we analyze large turbulence data sets from two different experiments. They consists of high quality, high sampling rate and long observation duration longitudinal Eulerian velocity signals measured with hot-wire anemometry techniques. The first set is obtained from a jet turbulence experiment, with approximate (Taylor scale based) Reynolds number $R_\lambda \simeq 580$, due to C. Baudet [29] The second data set consists of wind-tunnel turbulence (1995 campaign), with $R_\lambda \simeq 2000$, due to Y. Gagne. It is worth mentioning that these data sets consist of 79 and 24 million samples, respectively!

ESTIMATION PARAMETERS

The remaining estimation parameters are set to $b_j = 1$, $l = 2 \cdot N_\psi = 6$ and $R = 399$, $S = 50$, $\alpha = 0.05$. According to turbulence common understanding, the power law behavior associated with scale invariance takes place in the so called inertial range of scales, which spreads from above the Taylor scale to below the integral scale, which are estimated at (in sample numbers) 2^6 and 2^{13} for the Jet data set and 2^4 and 2^{13} for the Wind-Tunnel, respectively. Careful analysis of the structure functions (as those in Figure 2) leads to the choices $[j_1, j_2] = [9, 13]$ for the Jet data set and $[j_1, j_2] = [6, 10]$ for Wind-Tunnel data set. In Turbulence analysis, selecting the regression range is, in itself an issue, which is not further discussed here.

RESULTS

From the structure functions [cf. Figure 2 (top row)], estimates for the multifractal attributes $\zeta(q), D(h), c_p$, computed from a single run with $n = 2^{20}$, are shown together with their 95% percentile confidence intervals (second and third row). Estimates and confidence intervals confirm that the data are multifractal: $\zeta(q)$ is not a linear function of q, the multifractal spectrum $D(h)$ has support on an whole range of Hölder exponents h, and the confidence interval for c_2 excludes the 0 value.

Wavelet leader-based estimates for c_1, c_2, c_3 averaged across the entire data sets for both Jet and Wind Tunnel turbulence are reported in Table 3, together with their bootstrap-based confidence intervals. It shows that confidence limits based on percentile or studentized statistics are extremely close. Furthermore, it indicates that the estimated c_ps are close but not equal for the two data sets. This can be either due to difficulties in the regression range selection or to the difference in Reynolds numbers (and can hence be related to the much debated issue in turbulence of universal values for multifractal attributes at infinite Reynolds numbers, [9]).

The leader bootstrap-based hypothesis tests on $c_2 = 0$ yield unambiguous results. Both data sets reject monofractality, with extremely low p-values (0.005), for both percentile and studentized tests. This is consistent with results in Table 3 where confidence intervals for c_2 clearly exclude the 0 value. Hence, this confirms that turbulence data select multifractal models rather than monofractal ones.

Table 4 shows the results of the leader bootstrap-based hypothesis tests on $c_3 = 0$. For both data sets, only a low fraction of the runs reject the hypothesis $c_3 = 0$. The corresponding p-values remain large, indicating a strong risk of incorrectly rejecting $c_3 = 0$. Percentile and studentized statistics-based tests are in good agreement. This is consistent with results in Table 3 where confidence intervals for c_3 do include the 0 value. Note that the estimates for c_3 are in agreement with value 0 up to the fourth digit for both data sets, as opposed to results for c_1 and c_2 that slightly differ from one data set to the other. The numerical simulations reported previously clearly indicate that nonzero c_3 values can be estimated from data. Moreover, they show that the tests possess satisfactory power even for small $c_{3,A}$ when only $n = 2^{15}$ samples are available, as opposed to the many $n = 2^{20}$ samples of the turbulence data sets used here. Therefore, the results reported in this article are strongly in favor of the conclusion that turbulence c_3 can be considered to be practically zero. The remainder of Table 4 indicates that both data sets strongly reject both the c_2 and c_3 of the She-Lévêque log-Poisson model while those of the log-normal Obukhov-Kolmogorov 62 are clearly preferred. The c_2 and c_3 values of the former are rejected for almost all runs for both data sets and both by percentile and studentized bootstrap tests with very small p-values, whereas the c_2 and c_3 of the latter are rejected for only a small fraction of runs and have large p-values. Our major conclusion—$c_3 = 0$—is in agreement with results reported in [30], confirming and strengthening them by the analysis of two different major turbulence data sets and by the use of a better mathematically grounded tool (wavelet leader) and of a statistically more meaningful (bootstrap confidence intervals and hypothesis tests) framework. From our point of view, it is an absolutely remarkable fact that the Obukhov-Kolmogorov 62 model, one of the oldest and mostly based on a

[TABLE 4] TESTING THE LOG-NORMAL AND THE LOG-POISSON MODELS. JET AND WIND TUNNEL TURBULENCE WAVELET LEADER-BASED BOOTSTRAP HYPOTHESIS TESTS FOR THE c_2 AND c_3 OF THE LOG-NORMAL (LN) AND LOG-POISSON (LP) MODELS (AVERAGE OVER RUNS, SIGNIFICANCE $\alpha = 0.05$).

	JET TURBULENCE DATA		WIND TUNNEL DATA	
MODEL: LN	$c_{2,0}$	$c_{3,0}$	$c_{2,0}$	$c_{3,0}$
	−0.0250	0.0000	−0.0250	0.0000
REJECT_{per}	42.5%	18.8%	16.6%	20.8%
REJECT_{stu}	40.0%	15.0%	8.3%	20.8%
P-VALUE_{per}	0.23	0.36	0.43	0.33
P-VALUE_{stu}	0.22	0.37	0.47	0.36
MODEL: LP	$c_{2,0}$	$c_{3,0}$	$c_{2,0}$	$c_{3,0}$
	−0.0365	0.0049	−0.0365	0.0049
REJECT_{per}	98.8%	95.0%	100%	95.8%
REJECT_{stu}	98.8%	87.5%	100%	87.5%
P-VALUE_{per}	0.005	0.009	0.005	0.034
P-VALUE_{stu}	0.005	0.026	0.005	0.043

law of large number argument, is consistently preferred by data against the numerous declinations proposed since and elaborated from potentially more relevant physical arguments.

AUTHORS

Herwig Wendt (herwig.wendt@ens-lyon.fr) received the M.S. degree in electrical engineering and telecommunications from Vienna University of Technology, Austria, in 2005. He is currently working toward the Ph.D. degree in physics and signal processing at the Laboratoire de Physique at Ecole Normale Supérieure de Lyon, France. His research interests include scale invariance phenomena, point processes, extreme values, bootstrap methods, and machine learning.

Patrice Abry (patrice.abry@ens-lyon.fr) received the degree of Professeur-Agrégé de Sciences Physiques, in 1989 at Ecole Normale Supérieure de Cachan and completed a Ph.D. in physics and signal processing at Université Claude-Bernard Lyon I in 1994. Since October 1995, he is a permanent CNRS researcher, at the Laboratoire de Physique of Ecole Normale Supérieure de Lyon. He received the AFCET-MESR-CNRS prize for best Ph.D. in signal processing for the years 1993–1994. He is the author of the book *Ondelettes et Turbulences—Multirésolution, Algorithmes de Décompositions, Invariance d'échelle et Signaux de Pression*, published in Diderot, Paris, France, in 1997 and also the coeditor of a book in French titled *Lois d'échelle, Fractales et Ondelettes*, Hermés, Paris, France, 2002. His current research interests include wavelet analysis of scaling processes (self-similarity, stable processes, multifractal, 1/f processes, long-range dependence, local regularity of processes, infinitely divisible cascades), mainly hydrodynamic turbulence and Internet traffic. He is a Member of the IEEE.

Stéphane Jaffard (jaffard@univ-paris12.fr) graduated at Ecole Polytechnique in 1984 and received a Ph.D. in mathematics (wavelet decompositions) in 1989. Since September 1995, he is Professor at the University Paris 12 in Créteil. He was a member of the Institut Universitaire de France from 2000–2005. He is coauthor of the book *Wavelets: Tools for Science and Technology* (SIAM, 2001). He is a member of the editorial boards of *Applied and Computational Harmonic Analysis*, *Journal of Fourier Analysis and its Applications*, and *Constructive Approximation*. His current research interests include Fourier series, Wavelet analysis, pointwise smoothness, multifractals, and stochastic processes.

RERERENCES

[1] B.B. Mandelbrot, "Intermittent turbulence in self similar cascades: Divergence of high moments and dimension of the carrier," *J. Fluid. Mech.*, vol. 62, no. 2, p. 331, 1974.

[2] G. Samorodnitsky and M. Taqqu, *Stable Non-Gaussian Random Processes.* New York: Chapman & Hall, 1994.

[3] R.H. Riedi, "Multifractal processes," in *Theory and Applications of Long Range Dependence,* P. Doukhan, G. Oppenheim, and M.S. Taqqu, Eds. Cambridge, MA: Birkhäuser, 2003.

[4] P. Abry, P. Flandrin, M. Taqqu, and D. Veitch, "Wavelets for the analysis, estimation and synthesis of scaling data," in *Self-similar Network Traffic and Performance Evaluation*, K. Park and W. Willinger, Eds. New York: Wiley, 2000.

[5] J. Istas and G. Lang, "Quadratic variations and estimation of the local Hölder index of a Gaussian process," *Annales de l'institut Henri Poincaré (B) Probabilités et Statistiques*, vol. 33, no. 4, pp. 407–436, 1997.

[6] J.-F. Coeurjolly, "Estimating the parameters of a fractional brownian motion by discrete variations of its sample paths," *Stat. Inference Stochastic Processes*, vol. 4, no. 6, pp. 199–227, 2001.

[7] D. Veitch and P. Abry, "A wavelet-based joint estimator of the parameters of long-range dependence," *IEEE Trans. Inform. Theory*, vol. 45, no. 3, pp. 878–897, 1999.

[8] H. Wendt and P. Abry, "Multifractality tests using bootstrapped wavelet leaders," *IEEE Trans. Signal Processing*, to be published.

[9] U. Frisch, *Turbulence: The Legacy of A.N. Kolmogorov.* Cambridge, U.K.: Cambridge Univ. Press, 1995.

[10] S. Jaffard, "Wavelet techniques in multifractal analysis," in *Fractal Geometry and Applications: A Jubilee of Benoît Mandelbrot,* M. Lapidus and M. van Frankenhuijsen, Eds., in *Proc. Symposia Pure Mathematics*, 2004, vol. 72, no. 2, American Mathematical Society, pp. 91–152.

[11] S. Jaffard, B. Lashermes, and P. Abry, "Wavelet leaders in multifractal analysis," in *Wavelet Analysis and Applications,* T. Qian, M.I. Vai, X. Yuesheng, Eds. Cambridge, MA: Birkhäuser, 2006, pp. 219–264.

[12] S. Mallat, *A Wavelet Tour of Signal Processing*. San Diego, CA: Academic, 1998.

[13] G. Parisi and U. Frisch, "On the singularity structure of fully developed turbulence, appendix to fully developed turbulence and intermittency by U. Frisch," in *Proc. Int. Summer School Physics Enrico Fermi,* Amsterdam: North Holland, 1985, pp. 84-88.

[14] B. Castaing, Y. Gagne, and M. Marchand, "Log-similarity for turbulent flows," *Physica D*, vol. 68, no. 3-4, pp. 387–400, 1993.

[15] J. Delour, J.F. Muzy, and A. Arneodo, "Intermittency of 1d velocity spatial profiles in turbulence: A magnitude cumulant analysis," *Europhys. J. B*, vol. 23, no. 2, pp. 243–248, 2001.

[16] E. Bacry, A. Arneodo, and J.F. Muzy, "Singularity spectrum of fractal signals from wavelet analysis: Exact results," *J. Stat. Phys.*, vol. 70, no. 3-4, pp. 635–674, 1993.

[17] A. Chhabra, C. Meneveau, R.V. Jensen, and K.R. Sreenivasan, "Direct determination of the singularity spectrum and its application to fully developed turbulence," *Phys. Rev. A, Gen. Phys.*, vol. 40, no. 9, pp. 5284-5294, 1989.

[18] B. Efron, *The Jackknife, the Bootstrap, and Other Resampling Plans*. Philadelphia, PA: SIAM, 1982.

[19] P. Hall, *The Bootstrap and Edgeworth Expansion*. New York: Springer-Verlag, 1992.

[20] S.N. Lahiri, *Resampling Methods for Dependent Data*. New York: Springer-Verlag, 2003.

[21] E.L. Lehmann, *Testing Statistical Hypotheses*. New York: Wiley, 1959.

[22] P. Hall and S.R. Wilson, "Two guidelines for bootstrap hypothesis testing," *Biometrics*, vol. 47, no. 2, pp. 757–762, 1991.

[23] A.C. Davison and D.V. Hinkley, *Bootstrap Methods and Their Application* (Cambridge Series on Statistical and Probabilistic Mathematics). Cambridge, U.K.: Cambridge Univ. Press, 1997.

[24] A.M. Zoubir and D.R. Iskander, *Bootstrap Techniques for Signal Processing.* Cambridge, U.K.: Cambridge Univ. Press, 2004.

[25] E. Bacry and J.F. Muzy, "Multifractal stationary random measures and multifractal random walks with log-infinitely divisible scaling laws," *Phys. Rev. E, Stat. Phys. Plasmas Fluids Relat.,* vol. 66, no. 5, p. 056121, 2002.

[26] P. Chainais, R. Riedi, and P. Abry, "On non scale invariant infinitely divisible cascades," *IEEE Trans. Inform. Theory*, vol. 51, no. 3, pp. 1063-1083, Mar. 2005.

[27] U. Frisch and G. Parisi, "Fully developed turbulence and intermittency," in *Proc. Int. Summer School Turbulence Predictability Geophysical Fluid Dynamics Climate Dynamics*, 1985, pp. 84–88.

[28] A.S. Monin and A.M. Yaglom, *Stat. Fluid Mechanics*. Cambridge, MA: MIT Press, 1975.

[29] G.R. Chavarria, C. Baudet, and S. Ciliberto, "Hierarchy of the energy dissipation moments in fully developed turbulence," *Phys. Rev. Lett.*, vol. 74, no. 11, pp. 1986–1989, 1995.

[30] A. Arneodo, S. Manneville, and J.-F. Muzy, "Towards log-normal statistics in high Reynolds number turbulence," *Eur. Phys. J. B*, vol. 1, no. 1, pp. 129–140, 1998. SP